

SYNTHESIS, CHARACTERIZATION AND CATALYTIC UTILIZATION OF A FERROCENE DIAMIDODIPHOSPHANEPetr ŠTĚPNIČKA^{a1,*}, Jiří SCHULZ^a, Ivana ČISAŘOVÁ^a and Karla FEJFAROVÁ^b^a Department of Inorganic Chemistry, Faculty of Science, Charles University, Hlavova 2030, 128 40 Prague 2, Czech Republic; e-mail: ¹ stepnic@natur.cuni.cz^b Institute of Physics, Academy of Sciences of the Czech Republic, Na Slovance 2, 182 21 Prague 8, Czech Republic

Received December 21, 2006

Accepted February 8, 2007

Dedicated to Dr Karel Mach on the occasion of his 70th birthday.

Amidation of 1'-(diphenylphosphanyl)ferrocene-1-carboxylic acid (Hdpf) with ethane-1,2-diamine afforded *N,N'*-ethylenebis[1'-(diphenylphosphanyl)ferrocene-1-carboxamide] (**1**), which was isolated in free and solvated form, 1·2AcOH. Both **1** and Hdpf were further converted to their respective phosphane sulfides, 2·2AcOH and **3** that were structurally characterized. Testing of the amidophosphane ligands in Suzuki–Miyaura cross-coupling reaction between phenylboronic acid and various aryl halides revealed that catalyst formed in situ from **1** and palladium(II) acetate is highly active in coupling reactions of aryl bromides whilst the corresponding aryl chlorides showed no or only poor conversions. The catalyst based on 2·2AcOH gave markedly lower yields of the coupling products.

Keywords: Ferrocene; Phosphines; Amides; Suzuki–Miyaura cross-coupling; Crystal structure determination; Ligands; X-ray diffraction.

In 1996, we reported the synthesis of the first phosphanylferrocene-carboxylic acid¹, 1'-(diphenylphosphanyl)ferrocene-1-carboxylic acid: Ph₂PfcCO₂H (Hdpf; fc = ferrocene-1,1'-diyl)². Since then, we have synthesized several other phosphanylferrocenecarboxylic ligands and studied their coordination chemistry, catalytic properties and utilized these compounds as organometallic synthons³. The last approach, for instance, ensued in the discovery of an alternative route to C-chiral phosphanylferrocenyl oxazolines⁴ and preparation of P-chelated ferrocene aminocarbenes⁵. The broad applicability of the involved Hdpf-amide intermediates prompted our interest in the phosphanylferrocenylamides and their possible catalytic use.

It has to be noted that several ferrocene amidophosphanes have been already reported in the literature. The prominent examples include com-

pounds obtained by directed ortho-lithiation of tertiary ferrocenecarboxamides⁶. Phosphanylferrocenylcarboxamides also served as key intermediates in the synthesis of ferrocenyloxazolines⁷, and have been tested as ligands and redox- and NMR-responsive receptors for inorganic anions⁸, ligands capable of stabilizing Pd(0), ligands for Heck reaction and as macrocyclic hosts for barbital⁹. In addition, there have been also reported some bis(phosphanylferrocene) diamides¹⁰ analogous to Trost's "chiral pocket" ligands¹¹.

Amidation of ferrocenecarboxylic and ferrocene-1,1'-dicarboxylic acids with dendritic amines has been used in the preparation of ferrocenylated dendrimers¹². A complementary approach based on the reaction of chiral ω -(ferrocenylsilyl)amines with polycarboxylic acids has been used in the synthesis of dendritic molecules with chiral ferrocene termini¹³. Finally, amides derived from chiral ferrocene amines have been used in the preparation of immobilized catalysts by means of anchoring of suitably substituted, chiral ferrocene derivatives onto solid supports¹⁴.

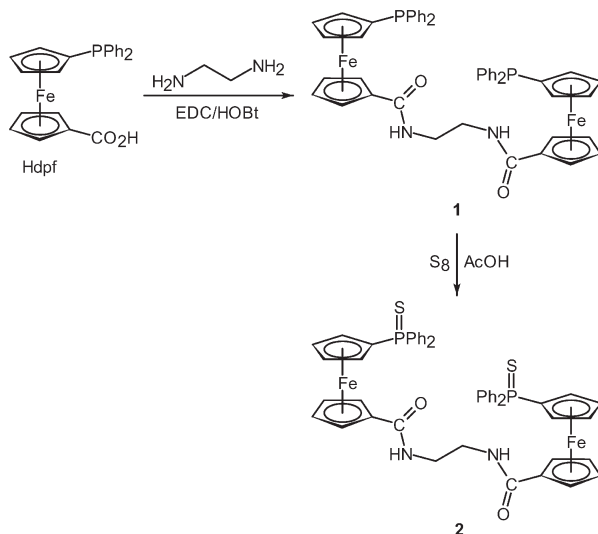
In this contribution we report about the preparation and structural characterization of a bis(phosphanylferrocene) diamide and its corresponding phosphane sulfide. We also present results of testing of the phosphanyl-amide ligands in palladium-catalyzed Suzuki-Miyaura reaction.

RESULTS AND DISCUSSION

Syntheses and Characterization

In the synthesis of diamide **1** (Scheme 1), we made use of the standard peptide coupling protocol¹⁵: Hdpf was first reacted in dichloromethane with 1-hydroxybenzotriazole (HOBt) and *N*-[3-(dimethylamino)propyl]-*N'*-ethylcarbodiimide (EDC) to give non-isolated benzotriazolyl ester¹⁶, which afforded the diamide upon addition of ethane-1,2-diamine. Notably, the diamide resulted exclusively even at Hdpf/diamine molar ratios lower than two, which indicates the preference of double acylation over monoamidation. Hence, a stoichiometric excess of the diamine could be used to avoid a loss of the ferrocene precursor without lowering the selectivity of the reaction. For instance, at a 1:1 Hdpf-to-diamine molar ratio, diamide **1** was isolated in 83% yield as an orange microcrystalline solid after standard aqueous work-up and column chromatography. The compound thus obtained was sufficiently pure but was further purified by crystallization from aqueous acetic acid whereupon the compound crystallized either

unsolvated (from dilute acid solutions) or in a better crystalline, solvated form **1**·2AcOH (from solutions with higher acetic acid contents).



SCHEME 1

Diamide **1** was further converted to its corresponding phosphane sulfide **2** by reacting with excess elemental sulfur in refluxing acetic acid (Scheme 1). Slow cooling of the reaction mixture gave analytically pure, crystalline solvate **2**·2AcOH in 88% yield. 1'-(Diphenylthiophosphoryl)ferrocene-1-carboxylic acid, Ph₂P(S)fcCO₂H (**3**), was prepared similarly as a model compound for a structural comparison. All compounds were characterized by elemental analysis and by NMR and IR spectra. Besides, the solid-state structures of **2**·2AcOH and **3** were determined by single-crystal X-ray diffraction analysis.

Solid-State Structures of **2**·2AcOH and **3**

The molecular structure of **2**·2AcOH is shown in Fig. 1 and the selected geometric data are listed in Table I. The solvated diamide crystallizes with the symmetry of the triclinic space group *P*-1̄ so that the midpoint of the ethane-1,2-diyl group connecting the amidoferrocene moieties coincides with the crystallographic inversion centre, which renders only the half of the diamide molecule and one molecule of the solvent symmetrically independent. Consequently, the ethane-1,2-diyl bridge shows ideal anti-periplanar conformation at the C(24)–C(24ⁱ) bond. A similar arrangement

has been observed in crystals of the related organic diamide, *N,N'*-ethylene-diacetamide¹⁷.

The amide moiety {C(6),C(11),N,O} in the molecule of **2** is practically planar and almost coplanar with its parent cyclopentadienyl ring, Cp(2), as evidenced by the perpendicular distance of C(24) atom from the amide plane of 0.038(2) Å and the dihedral angle of the amide and Cp(2) planes, which is only 3.0(1)°. Notably, the C=O bond length in **2**·2AcOH differs only little from that in Hdpf (cf. 1.229(7) and 1.228(6) Å for two Hdpf molecules within the asymmetric unit at room temperature)².

The geometry of the disubstituted ferrocene unit (fc) is quite regular, showing practically identical Fe-ring centroid distances. The cyclopentadienyl rings are tilted by 2.2(1)° and, as indicated by the torsion angle C(1)–Cg(1)–Cg(2)–C(6) = 131°, adopt an intermediate conformation between anti-eclipsed and anti-staggered (see Table I for definitions). The geometry of phosphorus substituent, particularly the P=S bond length, compares favourably with that in other structurally characterized, diphenylthiophosphoryl-substituted ferrocenes¹⁸.

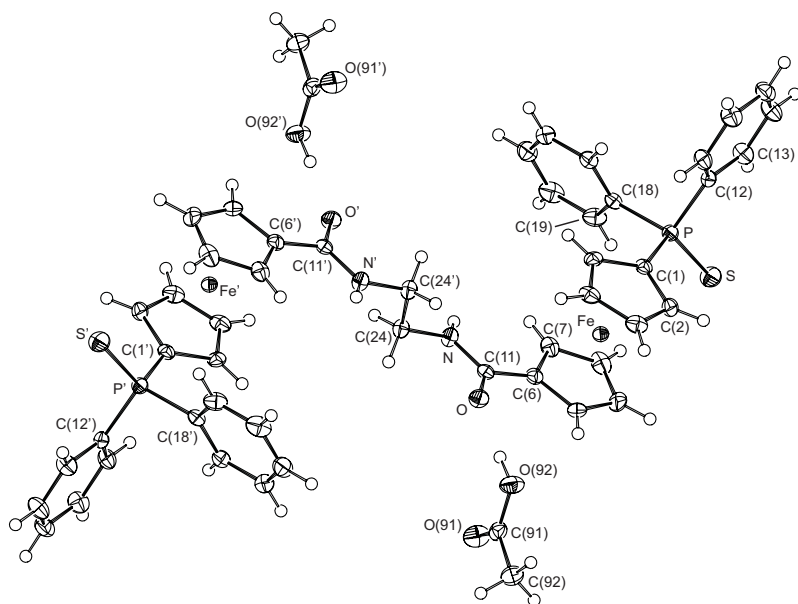


FIG. 1

PLATON view of the molecular structure of **2**·2AcOH showing the atom labeling scheme. The primed moiety is generated by the crystallographic inversion operation. Displacement ellipsoids are shown with 50% probability

Molecules of the diamide and the solvent in crystals of **2**·2AcOH associate predominantly through hydrogen bonds, forming an interesting, highly symmetric hydrogen-bonded assembly (Fig. 2, Table I). The adjacent *amide* units belonging to different *diamide* molecules are linked via hydrogen bonds to a pair of inversion-related molecules of the solvating acetic acid. The solvate molecules thus behave as molecular clamps giving rise to centrosymmetric, hydrogen-bonded macrocycles, where each amide moiety acts as a hydrogen donor through the NH group [N–H...O=C] and as hydrogen acceptor through the carbonyl group [C=O...H–O]. Since every diamide molecule is a part of two such macrocycles, the interplay of covalent and

TABLE I
Selected geometric data for **2**·2AcOH (in Å and °)^{a,b}

Molecular geometry			
Fe–Cg(1)	1.648(1)	∠Cp(1),Cp(2)	2.2(1)
Fe–Cg(2)	1.650(1)	∠Cp(2),{CCON}	3.0(1)
C(6)–C(11)	1.481(2)	C(6)–C(11)–O	121.4(2)
C(11)–O	1.243(2)	C(6)–C(11)–N	117.3(2)
C(11)–N	1.340(2)	O–C(11)–N	121.4(2)
N–C(24)	1.459(2)	C(11)–N–H(91)	119
C(24)–C(24')	1.532(2)	C(11)–N–C(24)	121.6(2)
P–S	1.953(1)	N–C(24)–C24 ^h	111.5(1)
P–C(1)	1.799(2)	O–C(11)–N–C(24)	0.8(2)
P–C(12)	1.816(2)	S–P–C ^c	112.10(6)–114.87(6)
P–C(18)	1.822(2)	C–P–C ^d	103.51(8)–106.42(8)
Hydrogen bond parameters ^e			
D–H...A	D–H	D...A	D–H...A
N–H(91)...O(91 ^h)	0.93	2.912(2)	164
O(92)–H(92)...O	0.96	2.632(2)	163

^a Symmetry operators used: *i* (1 – *x*, –*y*, 2 – *z*), *ii* (–*x*, –*y*, 2 – *z*). Note: Geometric data involving atoms in geometrically constrained positions are given without estimated standard deviations. ^b Least-squares planes are defined as follows: Cp(1), C(1–5); Cp(2), C(6–10); {CCON}, C(6), C(11), O, N. Cg(1) and Cg(2) denote the centroids of the cyclopentadienyl rings Cp(1) and Cp(2), respectively. Geometric data for the solvate molecule (in Å and °): C(91)–O(91) 1.206(2), C(91)–O(92) 1.327(2), C(91)–C(92) 1.495(3); O(91)–C(91)–O(92) 122.7(2), C(91)–O(92)–H(92) 111. ^c The range of S–P–C(1,12,18) angles. ^d The range of C(1)–P–C(12,18) and C(12)–P–C(18) angles. ^e D, donor; A, acceptor.

hydrogen bonds in conjunction with the crystallographic symmetry give rise to infinite linear arrays along the crystallographic axis *a*. The crystal assembly is further supported by relatively weaker C–H...O hydrogen bonds and graphite-like π – π stacking interaction of aromatic rings; the sulfur atoms do not exert any important intermolecular contacts.

The molecular structure of **3** is shown in Fig. 3 together with relevant geometric data. The structural parameters are roughly similar to those of the parent phosphane, Hd₂Pf^{2,19}. However, a notable difference can be found in the conformation of the ferrocene moiety, which is close to syn-eclipsed as evidenced by the torsion angle C(1)–Cg(1)–Cg(2)–C(6) of 63° (Hd₂Pf possesses an intermediate conformation between anti-eclipsed and anti-staggered with the torsion angle 162°). In addition, the carboxyl group is rotated from the plane of its cyclopentadienyl ring Cp(2), the dihedral angle of the {C(6),C(11),O(1),O(2)} and Cp(2) planes being 11.6(1)°. The C(6)–C(11) bond in **3** is slightly (but significantly with respect to estimated standard deviations) shorter than in **2·2AcOH** while exceeding the analogous distance in Hd₂Pf (1.442 Å on average).

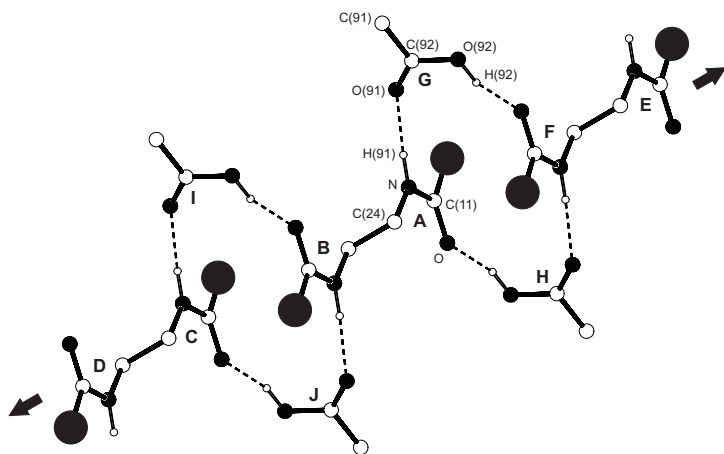


FIG. 2

A section of the hydrogen-bonded array in the structure of **2·2AcOH** showing hydrogen bonds as dashed lines. For clarity, only hydrogen bonded H-atoms are shown and the bulky 1'-(diphenylthiophosphoryl)ferrocene moieties are replaced with large black circles. The arrows indicate propagation direction of the infinite linear assembly. Symmetry codes: A (x, y, z), B ($1 - x, 2 - y, -z$), C ($-1 + x, y, z$), D ($-x, 2 - y, -z$), E ($1 + x, y, z$), F ($2 - x, 2 - y, -z$), G ($1 - x, 1 - y, -z$), H ($1 + x, 1 + y, z$), I ($-x, 1 - y, -z$), J ($x, 1 + y, z$)

Similarly to Hdpf, molecules of **3** in the crystal aggregate to centrosymmetric dimers via pairs of O–H...O hydrogen bonds with O...O separation of 2.651(2) Å and angles at the H atoms of 168 and 172° (Fig. 4). However, the acid hydrogen is observed disordered over two positions along the hydrogen bond line in the vicinity of both interacting oxygen atoms. The disorder which arises either from the carboxyl groups adopting two orientations rotated mutually by 180° (i.e., statistic disorder) or from the hydrogen atoms tunnelling between two equivalent energy minima, results in averaging of the C(11)–O(1,2) bond lengths. The C–O bond lengths differ by only 0.028 Å, which corresponds to ca. 2% of the mean bond distance (cf. ca. 7% for Hdpf). Crystal packing of the hydrogen-bonded dimers is supported by relatively weaker C–H... π -ring and offset π - π stacking interactions.

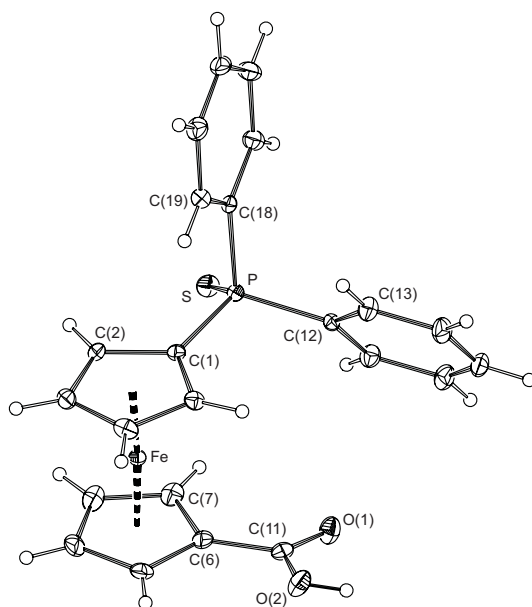


FIG. 3

PLATON view of the molecular structure of **3** showing the atom labeling scheme. For clarity, only one position of the disordered hydroxy proton is shown. Displacement ellipsoids correspond to the 30% probability level. Selected geometric data (in Å and °): Fe–Cg(1) 1.6413(9), Fe–Cg(2) 1.647(1), C(6)–C(11) 1.465(3), C(11)–O(1) 1.256(2), C(11)–O(2) 1.284(2), P–S 1.9525(7), P–C(1) 1.787(2), P–C(12) 1.811(2), P–C(18) 1.819(2), \angle Cp(1),Cp(2) 3.2(1), C(6)–C(11)–O(1) 119.3(2), S–P–C angles 113.06(6)–114.02(6), C–P–C angles 102.65(8)–108.22(8). The ring planes are defined as for **2**·2AcOH (see Table I)

TABLE II
Suzuki–Miyaura cross-coupling with amidophosphane ligands^a

Aryl halide (X/Y)	Conversion, %	
	L = 1	L = 2·2AcOH
Br/Me	99	43
Br/OMe	91	21
Br/COMe	100	89
Br/NO ₂	100	87
Cl/Me	0	– ^b
Cl/OMe	0	– ^b
Cl/COMe	0	– ^b
Cl/NO ₂	19	– ^b

^a See Scheme 2. Conditions: phenylboronic acid (1.2 mmol), aryl halide (1.0 mmol) and K₂CO₃ (2.0 mmol) were reacted in the presence of palladium(II) acetate (10 μmol, 1 mole %), the ligand (6 μmol) and diethylene glycol dimethyl ether as the internal standard (0.5 mmol) in dioxane (6 ml) at 90 °C for 20 h. Conversions were determined by integration of ¹H NMR spectra recorded for filtered reaction mixtures (see Experimental for details). The results are averages of two independent runs. ^b Not tested.

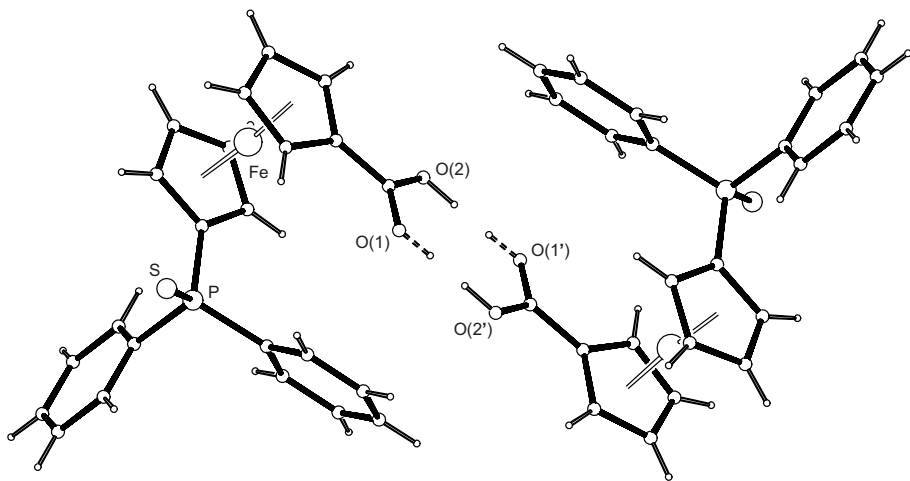
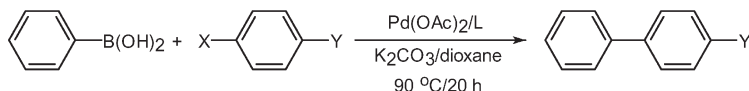


FIG. 4

View of the hydrogen bonded dimers in crystal of **3**. The primed atoms are generated by the (1 - x, 1 - y, 1 - z) symmetry operation

Catalytic Experiments

Catalytic activity of palladium-based systems based on the diamide ligands was assessed in Suzuki–Miyaura cross-coupling reactions²⁰ of phenylboronic acid with various aryl halides to give 4-substituted biphenyls (Scheme 2). The results are summarized in Table II.



SCHEME 2

Reactions performed in the presence of diamide **1**, 1 mole % palladium(II) acetate, and potassium carbonate as a base proceed with excellent conversions for all the aryl bromides tested. By contrast, the less reactive aryl chlorides²¹ did not react at all or with only poor conversion when strongly activated with an electron-withdrawing substituent (e.g., 4-O₂NC₆H₄Cl). Replacement of **1** with its corresponding phosphane sulfide **2** resulted in a significant drop of the observed conversions. Good yields of the coupling products were obtained only with activated aryl bromides while the non-activated substrates showed only moderate to poor conversions (4-MeOC₆H₄Br and 4-MeC₆H₄Br).

CONCLUSIONS

Amidation of ethane-1,2-diamine with Hd₂pf affords a ditopic ferrocene amidophosphane **1**, which can be isolated either unsolvated or in the solvated form (**1**·2AcOH) depending on the concentration of the acetic acid solvent during recrystallization. The role of the solvate in the crystal architecture was demonstrated by X-ray diffraction analysis of the solvated phosphane sulfide **2**·2AcOH. Testing of the diamides in Suzuki–Miyaura reaction showed the **1**–palladium(II) acetate catalytic system to efficiently promote the coupling of aryl bromides. The reactions involving the corresponding aryl chlorides did not proceed at all or with only low conversions in the case of activated substrates. Sulfidation at the phosphorus substituents strongly reduced activity of the catalytic system, which is particularly apparent in reactions with non-activated (electron-rich) aryl bromides.

EXPERIMENTAL

Syntheses were performed under argon atmosphere and with exclusion of the direct daylight. Hdpf was prepared by the literature procedure². Ethane-1,2-diamine was freshly distilled from little sodium. Toluene and dioxane were dried by standing over sodium metal and distilled. Dichloromethane was pre-dried with anhydrous potassium carbonate and distilled from calcium hydride. Solvents for chromatography and crystallizations were used as received from commercial sources (Merck, Lach-Ner).

Melting points were determined on a Kofler apparatus and are uncorrected. NMR spectra were measured on a Varian Unity Inova 400 spectrometer (¹H, 399.95; ¹³C, 100.58; ³¹P, 161.90 MHz) at 298 K. Chemical shifts (δ , ppm) are given relative to internal tetramethylsilane (¹H and ¹³C) or an external 85% aqueous H₃PO₄ (³¹P). Coupling constants, *J*, are given in Hz. IR spectra (ν , cm⁻¹) were recorded on an FT IR Nicolet Magna 760 instrument in the range 400–4000 cm⁻¹. Mass spectra were obtained on a ZAB-SEQ VG Analytical spectrometer.

Preparation of *N,N'*-Ethylenebis[1'-(diphenylphosphanyl)ferrocene-1-carboxamide] (**1**)

1-Hydroxybenzotriazole (810 mg, 6.0 mmol) was added to a solution of Hdpf (2.07 g, 5.0 mmol) in dry dichloromethane (30 ml). The mixture was cooled in an ice bath and treated with *N*-[3-(dimethylamino)propyl]-*N'*-ethylcarbodiimide (EDC; 950 mg, 6.0 mmol). The triazole quickly dissolved and the resulting orange red solution stirred at 0 °C for 30 min. Then, dry ethane-1,2-diamine (0.20 ml, 3.0 mmol) was added, causing an immediate precipitation. The mixture was stirred at room temperature overnight, and the reaction terminated by addition of 3 M HCl (10 ml) and stirring for another 10 min. The aqueous layer was discarded and the organic solution diluted with dichloromethane (up to ca. 170 ml), washed well with brine and dried over anhydrous MgSO₄. Subsequent evaporation afforded the crude product, which was purified by flash chromatography on a short silica gel column using a dichloromethane–methanol mixture (10:1 v/v) as the eluent. The single band eluted was collected, the eluate evaporated and the solid residue crystallized from hot, aqueous acetic acid (ca. 85%). The solvate 1·2AcOH formed after several days at +4 °C was filtered off and dried under vacuum. Yield 1.78 g (83%). Note: Lowering the acetic acid concentration in the crystallization results in the formation of solvent-free product. The amount of solvate can be easily checked by ¹H NMR spectroscopy. M.p. 95–97 °C. ¹H NMR (CDCl₃): 2.10 (s, 3 H, CH₃CO₂H); 3.47 (m, 2 H, NCH₂); 4.06 (apparent q, 2 H); 4.20 (apparent t, 2 H); 4.36 (apparent t, 2 H); 4.62 (apparent triplet, 2 H, 4 × CH of fc); 6.61 (br s, 1 H, NH); 7.26–7.38 (m, 10 H, PPh₂). ¹³C{¹H} NMR (CDCl₃): 20.82 (CH₃CO₂H); 40.49 (NCH₂); 69.43, 71.87, 72.91 (d, *J*_{CP} = 4); 74.33 (d, *J*_{CP} = 14, CH of fc); 76.12 (C-CO of fc); 128.27 (d, *J*_{CP} = 7); 128.71, 133.47 (d, *J*_{CP} = 20, CH of PPh₂); 138.41 (d, *J*_{CP} = 9, C-P of PPh₂); 171.58 (amide C=O); 176.34 (CH₃CO₂H); ³¹P{¹H} NMR (CDCl₃): -17.2 (s). IR (Nujol): 3305 vs, 1633 vs, 1585 w, 1545 vs, 1307 s, 1294 s, 1238 s, 1194 m, 1159 s, 1091 m, 1029 s, 999 w, 925 m, 852 w, 837 m, 814 m, 747 vs, 699 vs, 667 m, 637 m, 590 m, 522 m, 507 m, 498 vs, 490 vs, 451 m. For C₅₂H₅₀Fe₂N₂O₆P₂ (solvate 1·2AcOH) calculated: 64.21% C, 5.18% H, 2.88% N; found: 63.81% C, 5.17% H, 2.70% N.

Analytical data for unsolvated **2**. Solution NMR spectra of unsolvated **2** are virtually identical to those of the solvate, lacking the acetic acid resonances. IR (Nujol): 3422 m, 3331 s, 1716 s, 1653 vs, 1610 s, 1315 w, 1299 m, 1284 s, 1238 m, 1187 m, 1169 s, 1104 vs, 1071 m,

1033 m, 1026 m, 999 m, 840 s, 828 m, 763 s, 750 s, 714 vs, 700 m, 692 s, 651 vs, 632 m, 615 s, 569 m, 542 m, 525 s, 508 m, 487 vs, 468 m, 444 m, 421 m.

Preparation of *N,N'*-Ethylenebis[1'-(diphenylthiophosphoryl)ferrocene-1-carboxamide]-Acetic Acid (1:2) (**2·2AcOH**)

Diamide **1** (170.4 mg, 0.2 mmol), sulfur (16 mg, 0.5 mmol) and glacial acetic acid (10 ml) were heated at gentle reflux for 90 min. The solid reactants quickly dissolved to give a clear orange solution, which later deposited an orange precipitate. The solid formed was dissolved by addition of another acetic acid (3 ml), the solution was filtered while hot and allowed to crystallize by first slow cooling to room temperature and then storing overnight at +4 °C. The separated product was filtered off, washed with aqueous acetic acid (1:1) and water, and dried under vacuum to give **2·2AcOH** as a rusty brown microcrystalline solid. Yield 161 mg (88%).

Analytical data for **2·2AcOH**. M.p. > 145 °C (decomp.). ¹H NMR (CDCl₃): 2.10 (s, 3 H, CH₃CO₂H); 3.62 (m, 2 H, NCH₂); 4.04 (apparent t, 2 H); 4.29 (apparent q, 2 H); 4.54 (apparent q, 2 H); 4.86 (apparent t, 2 H, CH of fc); 7.26–7.74 (m, 11 H, CH of PPh₂ and NH). ¹³C{¹H} NMR (CDCl₃): 20.64 (CH₃CO₂H); 40.24 (NCH₂); 70.75, 71.74, 73.57 (d, *J*_{CP} = 10); 74.66 (d, *J*_{CP} = 12, CH of fc); 76.02 (d, ¹*J*_{CP} = 96, C-P of fc); 77.97 (C-CO of fc); 128.37 (d, *J*_{CP} = 13); 131.52 (d, *J*_{CP} = 3); 131.63 (d, *J*_{CP} = 11, CH of PPh₂); 133.64 (d, ¹*J*_{CP} = 87, C-P of PPh₂); 170.35 (amide C=O); 175.33 (CH₃CO₂H). ³¹P{¹H} NMR (CDCl₃): +39.4 (s). IR (Nujol): 3363 s, 1698 vs, 1605 vs, 1551 vs, 1299 m, 1265 br m, 1246 w, 1192 m, 1158 m, 1068 m, 1028 m, 891 w, 829 s, 748 s, 700 s, 668 m, 636 w, 616 w, 570 br m, 514 s, 503 s, 490 s, 477 w, 453 m, 429 w. For C₅₂H₅₀Fe₂N₂O₂P₂S₂ (solvate **2·2AcOH**) calculated: 60.24% C, 4.86% H, 2.70% N; found: 59.36% C, 4.59% H, 2.57% N.

Preparation of 1'-(Diphenylthiophosphoryl)ferrocene-1-carboxylic Acid (**3**)

Hdpf (104 mg, 0.25 mmol) and elemental sulfur (10 mg, 0.3 mmol) were dissolved in dry toluene (12 ml) and the solution was heated at reflux for 1 h. Then, the reaction mixture was cooled to room temperature, evaporated under reduced pressure and the brown residue was dissolved in hot ethyl acetate (12 ml). The solution was filtered and the filtrate overlaid with hexane (12 ml). Crystallization by diffusion at room temperature followed by cooling to -18 °C (several days) gave **3** as well-developed rusty brown crystals, which were isolated by suction, washed with pentane and dried under vacuum. Yield 96 mg (86%). M.p. darkens above ca. 200 °C (decomp.). ¹H NMR (CDCl₃): 4.51 (apparent t, 2 H); 4.53 (apparent q, 2 H); 4.57 (apparent q, 2 H); 4.78 (apparent t, 2 H, 4 × CH, fc); 7.40–7.75 (m, 10 H, PPh₂). ¹³C{¹H} NMR (CDCl₃): 71.03 (C-CO of fc); 72.03, 74.31 (d, *J*_{PC} = 2); 74.42 (d, *J*_{PC} = 5); 74.5 (4 × CH of fc); 77.33 (d, ¹*J*_{PC} = 96, C-P of fc); 128.34 (d, *J*_{PC} = 13); 131.46 (d, *J*_{PC} = 2); 131.59 (d, *J*_{PC} = 11, 3 × CH of PPh₂); 133.91 (d, ¹*J*_{PC} = 87, C-P of PPh₂); 175.45 (CO₂H). ³¹P{¹H} NMR (CDCl₃): +41.3 (s). IR (Nujol): 1674 s, 1296 s, 1168 m, 1101 m, 1027 m, 914 m composite, 839 m, 819 w, 747 m, 719 s, 691 m, 657 m, 658 w, 615 w, 558 w, 540 m, 515 w, 501 m, 485 s, 457 w, 442 w. For C₂₃H₁₉FeO₂PS (446.3) calculated: 61.90% C, 4.29% H; found: 61.93% C, 4.12% H.

TABLE III
Crystallographic data, data collection and structure refinement parameters for 2·2AcOH and 3

Compound	2·2AcOH	3
Formula	C ₅₂ H ₅₀ Fe ₂ N ₂ O ₆ P ₂ S ₂	C ₂₃ H ₁₉ FeO ₂ PS
<i>M</i> , g mol ⁻¹	1036.70	446.26
<i>T</i> , K	150(2)	150(2)
Crystal system	triclinic	monoclinic
Space group	<i>P</i> $\bar{1}$ (No. 2)	<i>P</i> 2 ₁ / <i>n</i> (No. 14)
<i>a</i> , Å	7.354(2)	13.4619(3)
<i>b</i> , Å	9.578(4)	9.3024(2)
<i>c</i> , Å	17.010(5)	16.3407(4)
α , °	96.75(3)	
β , °	93.84(2)	106.756(2)
γ , °	98.92(2)	
<i>V</i> , Å ³	1171.0(7)	1959.43(8)
<i>Z</i>	1	4
<i>D</i> , g ml ⁻¹	1.470	1.513
μ (MoK α), mm ⁻¹	0.831	0.974
<i>T</i> ^b	0.953–1.033	0.815–1.000
Diffractions total	15200	23186
Unique/observed ^c diffractions	4827/3707	4089/3234
<i>R</i> _{int} ^d , %	2.22	2.87
No. of parameters	301	254
<i>R</i> observed diffractions, % ^e	2.67	2.53
<i>R</i> , <i>wR</i> all data, % ^e	3.81, 7.03	3.63, 7.07
$\Delta\rho$, e Å ⁻³	0.40, -0.35	0.39, -0.21
CCDC reference No.	630145	630146

^a C₄₈H₄₂Fe₂N₂O₂P₂S₂·2C₂H₄O₂. ^b The range of transmission coefficients. ^c Diffractions with $I_o > 2\sigma(I_o)$. ^d $R_{int} = \sum |F_o^2 - F_c^2(\text{mean})| / \sum F_o^2$, where $F_o^2(\text{mean})$ is the average intensity for symmetry equivalent diffractions. ^e $R = \sum |F_o| - |F_c| / \sum |F_o|$, $wR = [\sum \{w(F_o^2 - F_c^2)^2\} / \sum w(F_o^2)^2]^{1/2}$.

Catalytic Tests

Palladium(II) acetate (10 μmol), the ligand (6 μmol of **1** or **2**, potassium carbonate (2.0 mmol), phenylboronic acid (1.2 mmol), and diethylene glycol dimethyl ether as internal standard (0.50 mmol, 1.0 ml of 0.5 M stock solution in dioxane) were mixed with dry dioxane (5 ml). The reaction vessel was flushed with argon and aryl halide (1.0 mmol) was introduced. Then, the reaction flask was sealed and kept at 90 °C (bath temperature) with stirring for 20 h. After cooling to room temperature, a portion of the liquid phase was filtered through a poly(tetrafluoroethylene) syringe filter (0.45 μm pore size) and analyzed by ^1H NMR spectroscopy. The results are summarized in Table II.

X-ray Crystallography

Crystals suitable for X-ray diffraction analysis were selected directly from the reaction batch (**3**: brown prisms, $0.17 \times 0.31 \times 0.76 \text{ mm}^3$) or grown by recrystallization from hot aqueous acetic acid (**2**·2AcOH: orange prisms, $0.02 \times 0.14 \times 0.35 \text{ mm}^3$). Full-set diffraction data ($\pm h \pm k \pm l$) were collected on an Oxford KM4 CCD diffractometer equipped with an Oxford Cryojet cooler (Oxford Instruments) using graphite-monochromatized $\text{MoK}\alpha$ radiation ($\lambda = 0.71073 \text{ \AA}$). The data were corrected for absorption by a numerical method based on multiply measured diffraction intensity as incorporated in the diffractometer software²². The range of the transmission factors and other relevant crystallographic data are given in Table III.

The structures were solved by direct methods (SIR97, ref.²³) and refined by full-matrix least-squares on F^2 (SHELXL97, ref.²⁴). The non-hydrogen atoms were refined with anisotropic displacement parameters. Hydrogen atoms at the NH and OH groups in **2**·2AcOH were located on the difference electron density maps and refined as riding atoms with unconstrained isotropic displacement parameters. The OH hydrogen in **3**, which participates in the usual dimer formation via $\text{O-H}\cdots\text{O}=\text{C}$ hydrogen bonding, appears disordered over two positions as if flipping between the OH group of one molecule and carbonyl oxygen of the other and vice versa. Both positions were clearly identified on the difference electron density maps, assigned $U_{\text{iso}}(\text{H}) = 1.2U_{\text{eq}}(\text{O})$, and refined as riding atoms with freely variable partial occupancy; their refinement converged to ca. 40:60. All other hydrogen atoms (i.e., aromatic CH, CH_2 , and CH_3) were included in the calculated positions and refined as riding atoms with $U_{\text{iso}}(\text{H})$ set to $1.2U_{\text{eq}}$ of their bonded carbon atoms. Geometric calculations were performed with a recent version of the Platon program²⁵.

CCDC 630145 (for compound **2**·2AcOH) and 630146 (for compound **3**) contain the supplementary crystallographic data for this paper. These data can be obtained free of charge via www.ccdc.cam.ac.uk/conts/retrieving.html (or from the Cambridge Crystallographic Data Centre, 12, Union Road, Cambridge, CB2 1EZ, UK; fax: +44 1223 336033; or deposit@ccdc.cam.ac.uk).

This work was financially supported by the Ministry of Education, Youth and Sports of the Czech Republic within the frame of the projects No. LC 06070 and MSM0021620857.

REFERENCES AND NOTES

1. For an introductory review dealing (in part) with phosphanylcarboxylic ligands, see: Bader A., Lindner E.: *Coord. Chem. Rev.* **1991**, *108*, 27.
2. Podlaha J., Štěpnička P., Císařová I., Ludvík J.: *Organometallics* **1996**, *15*, 543.
3. Štěpnička P.: *Eur. J. Inorg. Chem.* **2005**, 3787.
4. Drahoňovský D., Císařová I., Štěpnička P., Dvořáková H., Maloň P., Dvořák D.: *Collect. Czech. Chem. Commun.* **2001**, *66*, 588.
5. Meca L., Dvořák D., Ludvík J., Císařová I., Štěpnička P.: *Organometallics* **2004**, *23*, 2541.
6. a) Tsukazaki M., Tinkl M., Roglans A., Chapell B. J., Taylor N. J., Snieckus V.: *J. Am. Chem. Soc.* **1996**, *118*, 685; b) Laufer R. S., Veith U., Taylor N. J., Snieckus V.: *Org. Lett.* **2000**, *2*, 629; c) Metallinos C., Szillat H., Taylor N. J., Snieckus V.: *Adv. Synth. Catal.* **2003**, *345*, 370.
7. a) Sutcliffe O. B., Bryce M. R.: *Tetrahedron: Asymmetry* **2003**, *14*, 2297; b) Richards C. J., Locke A. J.: *Tetrahedron: Asymmetry* **1998**, *9*, 2377; c) For use of Hdpf in the synthesis of phosphanylferrocene oxazolines, see ref.⁴.
8. Kingston J. E., Ashford L., Beer P. D., Drew M. G. B.: *J. Chem. Soc., Dalton Trans.* **1999**, 251.
9. Sørensen H. S., Larsen J., Rasmussen B. S., Laursen B., Hansen S. G., Skrydstrup T., Amatore C., Jutand A.: *Organometallics* **2002**, *21*, 5243.
10. a) You S.-L., Hou X.-L., Dai L.-X., Cao B.-X., Sun J.: *Chem. Commun.* **2000**, 1933; b) You S.-L., Hou X.-L., Dai L.-X., Zhu X.-Z.: *Org. Lett.* **2001**, *3*, 149; c) You S.-L., Hou X.-L., Dai L.-X.: *J. Organomet. Chem.* **2001**, *637–639*, 762; d) Longmire J. M., Wang B., Zhang X.: *Tetrahedron Lett.* **2000**, *41*, 5435; e) Longmire J. M., Wang B., Zhang X.: *J. Am. Chem. Soc.* **2002**, *124*, 13400.
11. a) Trost B. M., Machacek M. R., Aponick A.: *Acc. Chem. Res.* **2006**, *39*, 747; b) Trost B. M., van Vranken D. L.: *Chem. Rev.* **1996**, *96*, 395.
12. a) Cardona C. M., McCarley T. D., Kaifer A. E.: *J. Org. Chem.* **2000**, *65*, 1857; b) Stone D. L., Smith D. K., McGrail P. T.: *J. Am. Chem. Soc.* **2002**, *124*, 856; c) Ashton P. R., Balzani V., Clemente-Léon M., Colonna B., Credi A., Jayaraman N., Raymo F. M., Stoddart J. F., Venturi M.: *Chem. Eur. J.* **2002**, *8*, 673; d) Daniel M.-C., Ruiz J., Blais J.-C., Daro N., Astruc D.: *Chem. Eur. J.* **2003**, *9*, 4371.
13. a) Köllner C., Pugin B., Togni A.: *J. Am. Chem. Soc.* **1998**, *120*, 10274; b) Schneider R., Köllner C., Weber I., Togni A.: *Chem. Commun.* **1999**, 2415.
14. Representative examples: a) Gotov B., Toma Š., Macquarrie D. J.: *New J. Chem.* **2000**, *24*, 597; b) Cvangroš J., Toma Š., Žembéřová M., Macquarrie D. J.: *Molecules* **2005**, *10*, 679.
15. Kraatz H.-B.: *J. Inorg. Organomet. Polym. Mater.* **2005**, *15*, 83.
16. The ester was isolated by column chromatography as an orange brown solid from the reaction mixture obtained in an attempted amidation of Hdpf with aniline in the presence of EDC/HOBt reagents and was characterized as follows. ¹H NMR (CDCl₃): 4.35 (apparent q, 2 H); 4.56 (apparent t, 2 H); 4.71 (apparent t, 2 H); 4.97 (apparent t, 2 H, 4 × CH of fc); 7.26–7.56 (m, 13 H, PPh₂ and C₆H₄); 8.08 (dt, J_{HH} = 8.4, ≈ 1, 1 H, C₆H₄). ³¹P{¹H} NMR (CDCl₃): -17.9 (s). GC-MS: m/z (relative abundance): 531 (89, M⁺), 505 (6), 503 (5, [M - N₂]⁺), 487 (18), 414 (54, Hdpf⁺), 397 (17), 386 (7), 370 (13), 363 (18), 321 (100, C₅H₄PPh₂OFe), 305 (34).
17. Navarro E., Alemán C., Puiggalí J.: *Macromolecules* **1998**, *31*, 408.

18. 1,1'-Bis(diphenylthiophosphoryl)ferrocene: a) Fang Z.-G., Hor T. S. A., Wen Y.-S., Liu L.-L., Mak T. C. W.: *Polyhedron* **1995**, *14*, 2403; b) Pilloni G., Longato B., Bandoli G., Corain B.: *J. Chem. Soc., Dalton Trans.* **1997**, 819; other compounds: c) Butler I. R., Cullen W. R., Herring F. G., Jagannathan N. R., Einstein F. W. B., Jones R.: *Inorg. Chem.* **1986**, *25*, 4534; d) Štěpnička P., Císařová I.: *New J. Chem.* **2002**, *26*, 1389; e) Štěpnička P., Císařová I.: *Organometallics* **2003**, *22*, 1728; f) Štěpnička P., Císařová I.: *Collect. Czech. Chem. Commun.* **2006**, *71*, 215.
19. The observed difference in the bond lengths can be attributed to the different temperatures at which the structures have been determined (150 K for **3** vs r.t. for Hdpf).
20. de Meijere A., Diederich F. (Eds.): *Metal-Catalyzed Cross-Coupling Reactions*, 2nd ed. Wiley-VCH, Weinheim 2004.
21. Littke A. F., Fu G. C.: *Angew. Chem., Int. Ed.* **2002**, *41*, 4176.
22. *Crysalis CCD* and *Crysalis RED* (both version 1.171.31.7). Oxford Diffraction, Abingdon (U.K.) 2006.
23. Altomare A., Burla M. C., Camalli M., Cascarano G. L., Giacovazzo C., Guagliardi A., Moliterni A. G. G., Polidori G., Spagna R.: *J. Appl. Crystallogr.* **1999**, *32*, 115.
24. Sheldrick G. M.: *SHELXL97, Program for Crystal Structure Refinement from Diffraction Data*. University of Göttingen, Göttingen 1997.
25. Spek A. L.: *Platon, A Multipurpose Crystallographic Tool*. Utrecht University, Utrecht 2003; and updates. Distributed via Internet; <http://www.cryst.chem.uu.nl/platon/>.